Pathogen Filtration, Heterogeneity, and the Potable Reuse of Wastewater

ARTICLE *in* ENVIRONMENTAL SCIENCE AND TECHNOLOGY · JUNE 2001

Impact Factor: 5.33 · DOI: 10.1021/es0010960 · Source: PubMed

4 AUTHORS, INCLUDING:

Stanley Grant
University of California, Irvine
77 PUBLICATIONS **2,061** CITATIONS
SEE PROFILE

Terese Olson
University of Michigan
28 PUBLICATIONS **1,091** CITATIONS
SEE PROFILE

Environ. Sci. Technol. **2001**, *35,* 1798−1805

Pathogen Filtration, Heterogeneity, and the Potable Reuse of Wastewater

JEREMY A. REDMAN,[†]
STANLEY B. GRANT,*[,†]
TERESE M. OLSON,[‡] AND
MARY K. ESTES[§]

Department of Chemical and Biochemical Engineering and Material Science, University of California, Irvine, California 92697, Department of Civil and Environmental Engineering, University of Michigan, Ann Arbor, Michigan 48109, and Division of Molecular Virology, Baylor College of Medicine, Houston, Texas 77030

Filtration is commonly employed in water and wastewater treatment to remove particles and reduce the concentration of microbial pathogens. All physical models of packed-bed filtration are based on a proportional relationship between particle removal per unit depth of bed and the local particle concentration, $dC/dz = -C/l$, where l is the filtration length scale. Although l is known to vary with time and filter depth for heterogeneous suspensions or "dirty" beds, this paper demonstrates that the filtration rates of even seemingly monodisperse particle suspensions under clean-bed filtration conditions cannot be described with a single filtration length scale. A new model is derived for particle filtration that accounts for heterogeneity at two different spatial scales. Heterogeneity at the scale of the pathogen and/or collector (microscale heterogeneity) leads to a slow power-law decay of contaminant concentration with distance, instead of the fast exponential decay predicted by the standard model. Heterogeneity at the filter scale (macroscale heterogeneity) provides another level of complexity that can be evaluated once microscale heterogeneity effects are characterized. This model for microscale and macroscale heterogeneous particle filtration is verified by filtration experiments on a recombinant analogue of the waterborne pathogen Norwalk virus.

Introduction

Water conservation is the only viable solution to the dual problem facing many communities in the United States of rapid population growth and diminishing water resources. One of the most controversial water conservation measures is potable reuse, in which the raw drinking water supply for a community is augmented with highly treated wastewater. An obvious concern associated with potable reuse is the possibility that microbial pathogens present in the wastewater may contaminate water supplies and cause outbreaks of gastrointestinal disease. To prevent this from happening, a recent report by the National Research Council recommends that wastewater reclamation facilities employ "multiple and independent barriers to chemical and microbiological contaminants" and that "barriers for microbiological contaminants should be more robust than those for forms of contamination posing less acute danger" (*1*).

Filtration is commonly employed in water and wastewater treatment facilities to remove particulate and microbial contaminants from water. The basic idea is simple: contaminants are caught as they flow through a filter either because they are too big to pass through the water-filled pores (physical filtration) or because they are captured on the surface of filter grains (surface filtration). Filtration can take the form of a unit treatment process specifically designed to achieve some degree of contaminant removal, or it can occur naturally when water flows through sediments and soils before entering the potable supply. In either case, a valid mathematical model of filtration kinetics is critically needed to evaluate filter performance and to design treatment systems that will meet or exceed mandated levels of pathogen removal. The microbial contaminants usually targeted for removal are the enteric viruses, bacteria, and parasitic protozoa that have a fecal−oral route of transmission (*2, 3*).

The standard deep-bed filtration model is premised on a simple first-order expression for the decline in contaminant concentration C with distance z: $dC/dz = -C/l$. In this formulation, the filtration length scale l is the reciprocal of the commonly used filter coefficient λ (*4*). The magnitude of the filtration length scale l depends on the mechanism of filtration (physical or surface filtration) and the material properties of both the filter and the contaminant (*5*). This first-order conceptualization of filtration is widely used to model particle filtration in laboratory-scale experiments, and it is routinely incorporated into more sophisticated mathematical models of the fate and transport of contaminant particles in porous media (*6−8*). The filtration length scale is often assumed to be constant in the initial or clean-bed stage of filtration—corresponding to conditions when the fractional surface coverage of the collectors is small. However, as particles accumulate on a collector, l can decrease due to filter ripening (*9−11*) or increase due to blocking or the "shadow" effect (*12−14*).

The standard deep-bed filtration model predicts that the concentration of fluid-phase and deposited particles decays exponentially with distance. Recent filtration studies involving the measurement of deposited microorganisms (including parasites, bacteria, and viruses), however, suggest that physical and/or surface-chemical particle heterogeneity leads to nonexponential decay in deposited particles (*15−18*). Nonexponential removal of the fluid-phase virus concentration has also been observed in column and field experiments (*19−26*).

Evidence collected over the past three decades suggests that although the filtration length scales obtained by fitting particle effluent concentrations are a function of solution and surface chemistry, the dependence on solution parameters cannot be predicted from a first-principle analysis of the interaction forces (*27, 28*). Microscale collector heterogeneity—including surface roughness and spatial distribution of charge—has been proposed to account for the large discrepancies between models and data (*29−33*).

In this study we examined the filtration of recombinant Norwalk virus (rNV) particles in packed columns of uniformly sized quartz sand. Norwalk virus (NV) and Norwalk-like viruses are responsible for >96% of outbreaks of nonbacterial gastroenteritis associated with contaminated food or water in the United States (*34−36*). These emerging human pathogens are difficult to study because they cannot be

* Corresponding author phone: (949) 824-7320; fax: (949) 824-2541; e-mail: sbgrant@uci.edu.
[†] University of California.
[‡] University of Michigan.
[§] Baylor College of Medicine.

10.1021/es0010960 CCC: $20.00
Published on Web 03/22/2001

cultivated in tissue culture or animal models and because relatively few particles are shed from humans during an active infection. Recent cloning efforts have led to the high-level expression of the capsid protein that forms the outer surface of NV (*37*). When this capsid protein is expressed in vitro, it spontaneously assembles into recombinant virus-like particles that are morphologically and antigenically indistinguishable from native NV (*38*−*43*). From our perspective, the recombinant particles are an ideal experimental system because (i) the external structures of rNV and NV particles are apparently identical so they should behave similarly during filtration, (ii) the rNV particles can be grown to high concentration (20 mg of protein or $\sim 10^{15}$ particles/200 mL of cell culture), and (iii) they can be radiolabeled for easy detection. The suitability of these particles for column filtration studies was demonstrated in a previous paper (*44*).

In this paper we propose a filtration model that accounts for the fact that particles in water and wastewater can exhibit a spectrum of affinities for the filter grains. This conceptually simple modification of the standard model leads to a new set of equations that predict a slow power-law decay in contaminant concentration with distance, compared to the fast exponential decay predicted by the standard model. In laboratory tests of the new model we find that even highly purified rNV particles have a sufficiently heterogeneous distribution of collection rates to yield power-law filtration in packed columns of uniform quartz grains.

Model Development

To account for heterogeneity, we define a particle filtration distribution (PFD) function $n(l,z)$ such that $n(l,z)\,dl$ represents the number of particles per unit fluid volume at depth z in a filter that have filtration length scales in the range from l to $l + dl$. The PFD characterizes the distribution of filtration length scales represented among the population of particles at any depth z in the filter. A distribution of filtration length scales might arise, for example, from variations in the size and electrostatic potential of the particles. Particles characterized by small filtration length scales will be rapidly captured on the filter grains, leaving behind in the pore fluid particles characterized by longer filtration length scales. In general, the PFD is likely to be influenced by physical and surface-chemical heterogeneity in the nature of both particles *and* collectors.

If each differential slice of the particle population obeys first-order filtration kinetics, then we can write $\partial n(l,z)/\partial z = -n(l,z)/l$, which, after integration, becomes $n(l,z) = n(l,0)\, e^{-z/l}$. This derivation assumes that steady-state conditions apply and that dispersive fluxes can be neglected. More complex expressions for the PFD can be developed if these assumptions are relaxed, as will be documented in a future study. The concentration of particles in the pore fluid at any depth z can be found by invoking the principle of linear superposition and integrating the PFD over all filtration length scales:

$$C(z) = \int_{l_{min}}^{l_{max}} n(\xi,0)\, e^{-z/\xi}\, d\xi \tag{1}$$

The variables appearing in this equation represent the concentration $C(z)$ of particles in the pore fluid (units of particles per unit fluid volume), the PFD at the entrance to the filter $n(\xi,0)$, the smallest (l_{min}) and largest (l_{max}) filtration length scales represented among the population of particles, and the integration variable ξ. The concentration of particles retained on the surface of the filter grains, $S(z)$ (units of particles per unit of dry weight of filter), is related to the concentration in the pore fluid $C(z)$ by mass balance:

$$u\frac{dC(z)}{dz} = -\frac{\rho_b S(z)}{t_0 \epsilon} \tag{2}$$

Combining eqs 1 and 2 and solving for $S(z)$, we arrive at the following expression for the concentration of particles retained within the filter as a function of depth:

$$S(z) = \frac{t_0 u \epsilon}{\rho_b} \int_{l_{min}}^{l_{max}} \frac{n(\xi,0)}{\xi}\, e^{-z/\xi}\, d\xi \tag{3}$$

The variables in eqs 2 and 3 represent the operation time t_0 of the filter, the interstitial velocity u of the pore fluid, and the filter's porosity ϵ and bulk density ρ_b.

In this study we consider two limiting cases for the PFD. In the first case, a single filtration length l characterizes all particle−collector interactions and, consequently, the PFD at the entrance of the filter is given by $n(\xi,0) = C(0)\delta(\xi - l)$, where $\delta(x)$ is Dirac's delta function. Substituting this choice of the entrance PFD into eqs 1 and 3 and choosing l_{min} and l_{max} such that $l_{min} < l < l_{max}$, we recover the exponential equations predicted by the standard filtration model:

$$C(z) = C(0)\, e^{-z/l} \tag{4a}$$

$$S(z) = \frac{t_0 u C(0) \epsilon}{l \rho_b}\, e^{-z/l} \tag{4b}$$

Hence, the standard deep-bed filtration equations can be viewed as a special case of our more general model; specifically, deep-bed filtration equations represent the limit at which the particles and collectors are homogeneous and a single filtration length scale completely characterizes the PFD. In the experiments described later we obtained experimental estimates for the filtration length scale l by substituting the normalized particle breakthrough concentration into a rearranged form of eq 4a, $l = -L/\ln[C(L)/C(0)]$, where $C(0)$ and $C(L)$ represent the concentration of particles in the filter influent and effluent, respectively, and L represents the length of the filter.

The opposite of a completely homogeneous system is one for which no characteristic filtration length scale can be identified within the limits imposed by l_{min} and l_{max}; that is, the PFD is "fractal". Scale-free or fractal phenomena are mathematically represented by power-law relationships (*45*). The entrance PFD for this fractal limit is therefore given by $n(\xi,0) = A\xi^{-a}$, where the premultiplier A and power-law exponent a are constants. Substituting this power law into eqs 1 and 3, we obtain a new set of equations for the filtration of particles with a fractal PFD:

$$C(z) = C(0) z^{-(a-1)} B(a-1, z, l_{min}, l_{max}, a), \quad a \neq 1 \tag{5a}$$

$$S(z) = \frac{t_0 u C(0) \epsilon}{\rho_b} z^{-a} B(a, z, l_{min}, l_{max}, a), \quad a \neq 1 \tag{5b}$$

where

$$B(m, z, l_{min}, l_{max}, a) = \frac{\Gamma(m, z/l_{max}, z/l_{min})(1-a)}{l_{max}^{1-a} - l_{min}^{1-a}}, \quad a \neq 1 \tag{5c}$$

The variable m in eq 5c is equal to $a - 1$ or a in eqs 5a and 5b, respectively, and $\Gamma(r,b_0,b_1)$ is the incomplete gamma function:

$$\Gamma(r, b_0, b_1) = \int_{b_0}^{b_1} t^{r-1}\, e^{-t}\, dt \tag{5d}$$

The function $B(m,z,l_{min},l_{max},a)$ is a very weak function of z if $l_{min} \ll z \ll l_{max}$ and $m > 0$. Consequently, the following two conclusions apply for the choice of a fractal PFD: (i) the concentration of particles in the pore fluid decays like a power law of depth $C \sim z^{-(a-1)}$ when $a > 1$ and $l_{min} \ll z \ll l_{max}$, and (ii) the concentration of particles trapped in the filter decays like a power law of depth $S \sim z^{-a}$ when $a > 0$ and $l_{min} \ll z \ll l_{max}$. Provided that $a > 0$ and the retention properties of the filter do not vary much with distance, this analysis predicts that the spatial distribution of retained particles is a sensitive measure of the microscale heterogeneity in the collection rates. If collection rates are uniform, then S will decay exponentially with depth. If the collection rates are fractally heterogeneous, S will decay like a power law of depth.

Estimating Model Parameters

To compare the fractal model of particle filtration with experimental data, values for the parameters in eqs 5a and 5b must be estimated. Some of these parameters [C(0), t_0, u, ϵ, and ρ_b] are either known or are readily measurable. The remaining parameters (a, l_{min}, and l_{max}) were estimated as follows. The value of a was estimated from the slope of a log−log plot of the retained particles $S(z)$ against depth z in the filter over the range of depths where the power law would be expected to apply (i.e., $l_{min} \ll z \ll l_{max}$). The parameter l_{min} was calculated by assuming that the smallest filtration length scale corresponds to the diffusion-limited deposition rate for the smallest particles (*46*, *47*)

$$l_{min} = \frac{2d_c}{3(1-\epsilon)\eta_0} \tag{6a}$$

where

$$\eta_0 = 4A_s^{1/3}\left[\frac{3\pi\mu d_c d_p u\epsilon}{kT}\right]^{-2/3} \tag{6b}$$

$$A_s = \frac{2(1-\gamma^5)}{2-3\gamma+3\gamma^5-2\gamma^6}, \quad \gamma = (1-\epsilon)^{1/3} \tag{6c}$$

The variable η_0 is the single collector removal efficiency and represents the frequency of particle−collector collisions, A_s is the Happel cell parameter (*48*), d_c and d_p are the diameters of the collectors and smallest particles, respectively, μ is dynamic viscosity, k is Boltzmann's constant, and T is temperature. Radiolabeled rNV particles were used for the filtration experiments conducted in this study. These particles are spherically shaped protein shells measuring 38 nm in diameter. The protein shells are made up of 180 copies of a single 58 kDa capsid protein that has an approximate diameter of 2 nm. Because single capsid protein molecules were present in the rNV particle preparations, we chose $d_p = 2$ nm for the smallest "particles" in our experiments. Values of l_{max} for each filter segment were determined by numerically solving for the root of eq 5b after substituting calculated or experimentally determined values of $S(z_i)$, z_i, a, l_{min}, t_0, u, $C(0)$, ϵ, and ρ_b. The variable $S(z_i)$ represents the measured concentration of retained rNV particles in the ith segment of the filter; the distance between the entrance of the filter and the midpoint of the ith segment is designated z_i. This approach yields a separate l_{max} value for each segment of the filter analyzed. These individual values of l_{max} were weight-averaged by the length of the segment to yield a final estimate for l_{max}. A different procedure was used to estimate l_{max} for the case of the presence of significant macroscale heterogeneity, as will be described later in the paper.

In comparing predicted and measured values of $S(z)$ and $C(z)$, it is important to keep in mind that the model assumes a perfect mass balance, whereas in reality only a portion of the particles that enter a filter are recovered on the sand and in the effluent. To account for the imperfect recovery of particles, we reduced the predicted effluent concentration of particles by an amount that would completely account for the imperfect recovery of particles. In particular, the modified effluent concentration was calculated as

$$C(L) = C^{mod}(L) - (1-R)C(0) \tag{7}$$

where $C^{mod}(L)$ represents the predicted breakthrough concentration for the model based on perfect mass balance and R is the fractional recovery of particles. The derivation of eq 7 is included in the Supporting Information for this paper.

Experimental Methods

Preparation of Norwalk Virus Particles. Radiolabeled rNV particles used in the filtration experiments and the "cold" rNV particles used in electrophoretic mobility measurements were prepared as described previously (*44*).

Water Sampling and Analysis. Wastewater samples were collected from the final effluent of the San Jose Creek Water Reclamation Plant, located in Los Angeles County, California. Deionized water (Milli-Q) and analytical grade NaCl, HCl, and NaOH were used to prepare a 0.01 M NaCl solution, which was equilibrated to approximately pH 7. Full details on the water sampling and the physical and chemical analyses of the samples are included in the Supporting Information.

Filtration Experiments. The quartz sand used in the filtration experiments was purchased from Unimin (New Canaan, CT), size fractionated by a wet sedimentation/flotation technique, and then cleaned to remove metal and organic contaminants (*49*, *50*). The cleaning steps included soaking the sand in 12 N HCl for at least 24 h, washing with deionized water (Milli-Q), and baking the sand overnight at 800 °C. Cleaned sand was stored under a vacuum. Before filtration experiments were conducted, the sand was rehydrated by boiling for at least 1 h in deionized water. The filtration experiments were carried out in 16 mm inner diameter adjustable bed height glass columns (Pharmacia LKB C16, Piscataway, NJ) by allowing the quartz sand to settle in deionized water. The packed columns were equilibrated by pumping (Pharmacia LKB P1 peristaltic pump) ~60 pore volumes of the sample water through the column prior to each filtration experiment. Filtration experiments were conducted by pumping a pulse of virus-laden solution (either wastewater or NaCl solution) through the column for 60 min, followed by a pulse of virus-free solution for at least 30 min. A valve was used to switch between virus-free and virus-laden solutions. Influent solutions were prepared by diluting radioactively labeled rNV particles directly into 250 mL of sample solution. Samples were collected from the influent solution at both the beginning and end of the experiment. Column effluent was collected in 3 min increments using an automatic fraction collector (Pharmacia LKB FRAC-200). Blank samples were collected from the column effluent prior to applying the initial virus-laden pulse, as well as from the non-virus-containing solutions. All samples were mixed with scintillation cocktail and analyzed for radioactivity with a Beckman LS6000IC scintillation counter (Beckman, Fullerton, CA).

Analysis of Quartz Fractions. Upon completion of each filtration experiment, the glass columns were partially disassembled and the free fluid at the top of the packed sand bed was siphoned away. Compressed air was used to force the packed bed out of the column assembly as an intact core, whereupon it was sectioned and dried overnight in a 40 °C oven. The sections were weighed, and ~1 g of quartz from each section was transferred to a scintillation vial, mixed with 10 mL of scintillation cocktail, and analyzed for radioactivity by scintillation counting. The coefficient of

TABLE 1. Physical and Chemical Parameters of Water Samples

parameter	wastewater	0.01 M NaCl
temperature (°C)	27.6 ± 0.4[a]	NA[b]
dissolved oxygen (mg/L)	4.23 ± 0.08[a]	ND[c]
specific conductivity (μS/cm)	1109 ± 11[a]	1124
pH	6.96 ± 0.03[a]	6.93
oxidation reduction potential (mV)	663 ± 15[a]	ND
total organic carbon (TOC) (mg/L-C)	8.5 ± 0.1	ND
UV_{254} absorbance	0.1167 ± 0.0001	ND
heterotrophic plate count (CFU/mL)	23	0
total dissolved solids (mg/L)	632	586
total suspended solids (mg/L)	12	0
electrophoretic mobility of rNV particles (μm/s)/(V/cm)	−0.74 ± 0.01	−0.70 ± 0.16

[a] Determined at time of sampling. [b] Not applicable. [c] Not determined.

TABLE 2. Experimental and Model Parameters for Packed-Bed Filtration Studies[a]

parameter	wastewater	0.01 M NaCl
filter length (cm), L	30.3	29.4
interstitial flow rate (m/min), u	0.031	0.031
influent virus concn (cpm/mL) (particles/mL), $C(0)$	1867.0 (2.4×10^{10})	5112.6 (6.5×10^{10})
av breakthrough concn (cpm/mL) (particles/mL), $C(L)$	415.3 (5.3×10^{9})	4297.9 (5.5×10^{10})
fractional recovery, R	0.79	0.93
power-law exponent, a	0.8	0.8
min filtration length scale (m), l_{min}	$10^{-2.88}$	$10^{-2.88}$
max filtration length scale (m), l_{max}	$10^{0.44}$	$10^{4.34}$
standard filtration length scale (m), l	N/A[b]	1.7

[a] The bulk density of the quartz was determined to be $\rho_b = 1.33$ g/cm^3. The packed bed porosity was estimated to be $\epsilon = 0.49 \pm 0.02$, and the average grain diameter, determined by sieve analysis, was $d_c = 222 \pm 32$ μm (*71*, *72*). The inner diameter of the column apparatus was 16 mm. [b] Not applicable.

variance between the weights of the analyzed subsections was <3%. The presence of quartz and wastewater organics did not interfere with the scintillation detection of the radiolabled particles, as was demonstrated by a control experiment in which a known quantity of radiolabeled rNV particles was added to quartz sections from a filter bed that had been previously equilibrated with wastewater.

Results and Discussion

Virus Filtration. Filtration experiments were carried out with two different sources of water: a 0.01 M NaCl electrolyte solution prepared in the laboratory, and treated wastewater obtained from the San Jose Creek Water Reclamation Plant in Los Angeles County, California. The physical−chemical nature of the wastewater and NaCl solution and the estimated model parameters for the two experiments are summarized in Tables 1 and 2, respectively. The breakthrough curves for the filtration experiments conducted with 0.01 M NaCl and treated wastewater are plotted in Figure 1A (squares and circles, respectively). The normalized steady-state breakthrough concentrations of rNV particles in the filter effluent are 0.84 ± 0.02 (NaCl) and 0.22 ± 0.01 (wastewater), implying that 16% (NaCl) and 78% (wastewater) of the rNV particles that enter the 30 cm filter are retained on the quartz grains. Electrokinetic measurements of the rNV particles (Table 1) indicate that they are negatively charged in both the wastewater and the 0.01 M NaCl solution, as is the quartz sand (*50*). Hence, rNV particle filtration occurs against a repulsive electrostatic barrier in these two experiments. The greater degree of filtration observed in the wastewater experiment cannot be explained by the rNV particle mobility, as measured values were similar in both the wastewater and NaCl solution.

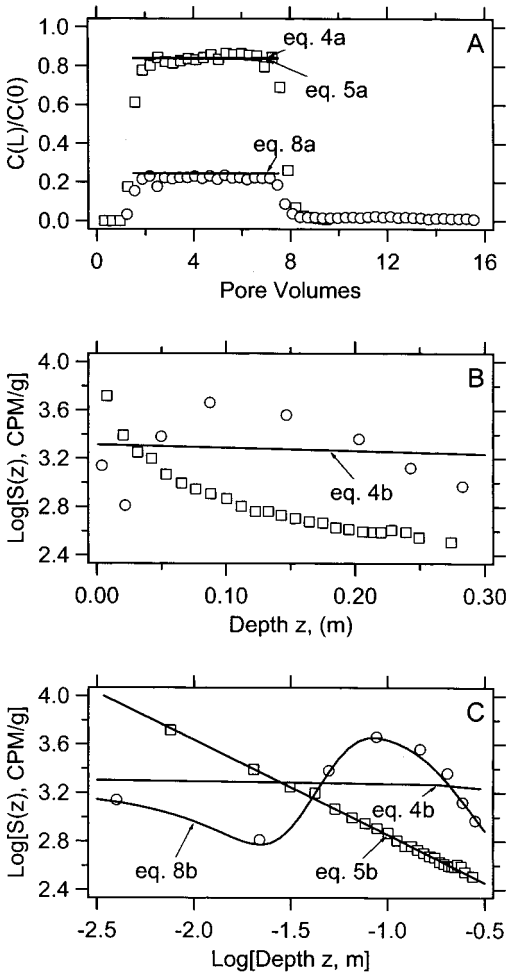

FIGURE 1. Breakthrough curves (A) and spatial distribution of retained particles (B and C) for filtration experiments conducted with 0.01 M NaCl electrolyte solution (□) and wastewater (○). Breakthrough curves were generated by dividing the concentration of rNV particles detected in the filter effluent $C(L)$ by the concentration in the influent $C(0)$ and then plotting this ratio against the number of pore volumes of water passed through the filter. Relevant physical and chemical characteristics of the experimental system are summarized in Tables 1 and 2. The solid lines represent model fits based on the standard first-order filtration model (eqs 4a and 4b), the microscale heterogeneity model (eqs 5a and 5b), and the macroscale heterogeneity model (eqs 8a and 8b). The lines corresponding to eqs 4a and 5a are indistinguishable in panel A.

Spatial Distribution of Attached Particles. The spatial distributions of retained particles are quite different for the two experiments (Figure 1B). The concentration of retained particles declines monotonically with depth when the pore fluid is 0.01 M NaCl. By contrast, the concentration of retained rNV particles achieves a maximum at a depth of ~10 cm

from the top of the filter when the pore fluid is wastewater. During the equilibration step that preceded the filtration experiment, dissolved organic carbon and suspended solids in the wastewater probably deposited near the top of the filter (TOC concentration in the wastewater is 8.5 mg/L, see Table 1). It has been argued that organic surface coatings block the deposition of particles by forming steric and/or electrostatic barriers (*22*, *51*), which would be consistent with decreased deposition of rNV particles near the filter entrance.

For the experiment conducted with 0.01 M NaCl, the retained rNV particle concentration falls along a nearly perfect line when plotted in a log−log format against depth (Figure 1C). Therefore, S decays like a power law of depth as predicted by our fractal PFD model. Indeed, this filtration model matches both the decay of S with depth (line labeled eq 5b in Figure 1C) and the steady-state effluent breakthrough level (line labeled eq 5a in Figure 1A), after accounting for the imperfect recovery of rNV particles (eq 7). *Importantly, the standard filtration model fails to describe the deposition pattern observed in these two experiments.* The standard model predicts that the retained particle concentration decays exponentially with depth, which would appear as a straight line if the data were plotted in a log−linear format. When S is plotted in this way, however, the data do not follow a linear trend (Figure 1B) and the predicted curve (labeled eq 4b in the figure) is a very poor fit to the observed data. Because the filtration length scale l in eqs 4a and 4b was determined from the steady-state portion of the breakthrough curve (see Model Development), the match between eq 4a and the data in Figure 1A is not significant.

The fact that our model predicts a power law for S is not a trivial consequence of assuming a power-law form for the particle distribution function $n(l,0)$. As described earlier, the power-law PFD represents a limiting case in which microscale heterogeneity leads to filtration length scales of all sizes between l_{min} and l_{max}. The surprising result here is that a power-law form of the PFD, which might be expected to apply to only the most heterogeneous of systems, appears to be a valid model for the filtration of highly purified particles in well-cleaned quartz grain media. Possible sources of this fractal heterogeneity are explored in the next section.

We also considered the possibility that the deposition pattern of rNV particles might be explained by blocking or ripening phenomena. The deposition profile obtained using an NaCl electrolyte pore fluid is inconsistent with a blocking mechanism, because there is no saturation front (i.e., the deposition profile declines monotonically with distance). Ripening, in which previously deposited particles accelerate subsequent deposition, might be consistent with the high concentration of particles observed near the entrance of the filter. However, there are several lines of evidence that suggest that ripening is not occurring in our system. First, ripening is typically observed when the influent contains relatively high particle concentrations (3−30 mg/L) (*10*, *52*), although it has been observed for more moderate particle concentrations such as the 1 mg/L employed in our experimental system (*53*). Second, most ripening studies involve either polydisperse systems consisting of many different types of suspended materials (e.g., wastewater) with particle diameters ranging from 0.3 to >100 μm (*54*−*56*) or systems that have been destabilized through the addition of polymer coagulant or divalent cations (*55*, *56*). In contrast, our experiments were conducted under repulsive conditions and utilized a simple NaCl electrolyte solution and a highly purified suspension of 38 nm diameter rNV particles. Third, there are no obvious mechanisms that would lead to filter ripening in our experimental system. Filter ripening is usually associated with large particles that become more efficiently strained out of solution as fines (or Schmutzedecke in the case of biofilms) deposit near the top of the filter. In our system, the rNV particles are not captured by straining but rather by diffusion onto the collector surface. One could conceive of a case in which positively charged protein debris possibly present in the rNV particle suspension is deposited onto the quartz grains, thereby creating favorable sites for rNV particle attachment. Even if this were the case, however, it is not clear that ripening would give rise to a power-law distribution of deposited particles, as observed in our experiments.

Origin of Microscale Heterogeneity. Because our NaCl data are best modeled with a fractal PFD, the following question arises: *In what respect are the rNV particle−collector interactions fractally heterogeneous?* Insight into this question can be obtained by considering the physical and chemical factors that control the surface filtration of rNV particles. The filtration length scale l should be inversely proportional to both the frequency with which the particles make contact with filter grains (η_0) and the probability that the particles will be captured on contact (α): $l \sim 1/(\eta_0\alpha)$. The only aspect of a Brownian particle that controls the frequency of contact is its radius (*5*): $\eta_0 \sim r^{-2/3}$. Electron micrographs of the rNV particle suspension showed that, after purification, the particle suspension consisted of single intact particles, although some partially assembled particles and protein debris almost certainly were present also. Assuming radii for the single capsid protein molecules and intact particles of 10 and 190 Å, respectively, η_0 should vary by no more than 1 $\log_{10}$ unit—far less than the 7 $\log_{10}$ unit difference between l_{min} and l_{max} estimated from the NaCl filtration experiment (see Table 2).

The probability of capture, on the other hand, depends exponentially on the potential energy barrier to deposition V_b (*57*): $\alpha \sim e^{-V_b/kT}$. Consequently, the value of α is quite sensitive to the detailed nature of the particle and the collector. A reasonable variation in the potential barrier V_b from 0 to 15 kT (*58*)—caused by heterogeneity in the electrostatic surface potential of rNV particles and the quartz sand, for example—would completely account for the 7 $\log_{10}$ unit range in the values of l_{min} and l_{max} observed here.

Macroscale Heterogeneity and a Filtration Model for Wastewater. As mentioned earlier, pre-equilibration with wastewater appears to reduce the rNV particle collection rates near the entrance to the filter. This spatial variation in collection rates, or "macroscale heterogeneity", can be modeled by several different approaches. One conceptually simple approach is to modify the filtration length scale for each differential slice of the particle population by a function $h(z)$ that varies with distance z in the filter: $\partial n/\partial z = -n/l^{eff}$, where $l^{eff} = l/h(z)$. Given this reformulation of the filtration kinetics, the equations for a fractal PFD become

$$C(z) = C(0)z^{-(a-1)}B(a-1,z,l^*_{min},l^*_{max},a) \qquad (8a)$$

$$S(z) = \frac{t_0 u C(0)\epsilon}{\rho_b}\left(\frac{z h(z)}{\tilde{H}(z)}\right)z^{-a}B(a,z,l^*_{min},l^*_{max},a) \qquad (8b)$$

$$l^*_{min} = l_{min} z/\tilde{H}(z) \qquad (8c)$$

$$l^*_{max} = l_{max} z/\tilde{H}(z) \qquad (8d)$$

$$\tilde{H}(z) = \int_0^z h(\xi)\, d\xi \qquad (8e)$$

The solutions for $C(z)$ and $S(z)$ with and without macroscale heterogeneity are nearly identical (compare eqs 8a and 8b with eqs 5a and 5b), except that in the macroscale heterogeneity model the parameter l_{min} is replaced with l^*_{min}, the parameter l_{max} is replaced with l^*_{max}, and the ratio

$z h(z)/\tilde{H}(z)$ appears on the right-hand side of eq 8b. If l_{min} represents the smallest filtration length scale that can be obtained in a system—as is the case in our study when l_{min} is calculated on the basis of a diffusion-limited deposition rate for the smallest particles (eq 6)—then the effective filtration length scale can never be smaller than l_{min}: $l^{eff} \geq l_{min}$. This inequality leads to the following constraint on the value of $h(z)$:

$$h(z) \leq 1 \tag{9}$$

The macroscale heterogeneity function $h(z)$ can be calculated from experimental measurements of the retained particle concentration as follows. Letting w_i and $S(z_i)$ represent, respectively, the dry weight of the ith segment of the filter and the measured concentration of retained particles in the ith segment, then the macroscale heterogeneity function $h(z_i)$ for the ith segment can be estimated by solving for the root of eq 10a:

$$z^{-(a-1)} B\left(a-1, z_i, \frac{l_{min} z_i}{\tilde{H}(z_i)}, \frac{l_{max} z_i}{\tilde{H}(z_i)}, a\right) = 1 - \sum_{j=1}^{i} \frac{S(z_i) w_j}{C(0) u \epsilon A_c t_0} \tag{10a}$$

$$\tilde{H}(z_i) = \sum_{j=1}^{i} h(z_i) \Delta_j \tag{10b}$$

Here, A_c represents the cross-sectional area of the filter, Δ_i represents the length of the ith segment, and all other variables have been defined previously. Equation 10a can be derived by solving the mass balance equation (eq 2) for $C(z)$, substituting eq 8a, and using the rectangular rule to numerically approximate the integral expressions (*59*). Before eq 10a can be solved, values for the parameters l_{min}, a, and l_{max} are needed. Following the procedure used to model the NaCl filtration data, the value of l_{min} was calculated from eq 6. As a first approximation, we assumed that the values of a were the same for the NaCl and wastewater experiments. Many of the power-law exponents that arise from the unsteady coagulation of particles are "universal", by which we mean that the exponent value does not depend on system details (*60*, *61*). Whether or not this concept of universality also applies to particle filtration, in general, and to the value of a, in particular, is an interesting issue for future research. Finally, the value of l_{max} was determined for the wastewater experiment such that the heterogeneity function $h(z)$ never violated the inequality given by eq 9; specifically, the value of l_{max} was adjusted so that the maximum value of $h(z)$ over the length of the filter was unity. Table 2 compares the l_{min}, l_{max}, and a values determined for the NaCl and wastewater experiments.

Values of $h(z)$ estimated from the deposition patterns of rNV particles are plotted in the top panel of Figure 2. As expected, $h(z)$ estimated for the NaCl data (squares in the top panel) are near unity over the length of the filter, implying that there is negligible macroscale heterogeneity in the collection rates for this particular experiment. In contrast, $h(z)$ values estimated from the wastewater data vary by 2 $\log_{10}$ units, from $\sim 10^{-2}$ to 1 at the inlet and outlet of the filter, respectively. In the context of our model, the effective maximum length scale, $l^{eff}_{max} = l_{max}/h(z)$, is a measure of the overall affinity of the particle population for the filter, similar in spirit to the attachment efficiency α that appears in deep-bed filtration theory (*5*). As particle deposition becomes more favorable, l^{eff}_{max} becomes smaller, and the total particle population is more rapidly filtered. The l^{eff}_{max} values calculated for the wastewater experiment are between 2 and 4 $\log_{10}$ units lower than the l^{eff}_{max} values calculated for the NaCl experiment (Figure 2B), implying that some component of the wastewater improves the overall filter performance near the exit of the filter. Moreover, the plot of l^{eff}_{max} for the wastewater experiment confirms the existence of significant spatial variability in the overall filtration rates, with the best filtration occurring near the exit of the filter where the values of l^{eff}_{max} are relatively small ($\sim$10 m). The mechanisms responsible for this spatial variability in deposition rates are currently unclear. As mentioned earlier, organic surface coatings of wastewater origin are a likely cause of the reduced filtration rates observed near the filter entrance. Blocking effects due to previously deposited wastewater particulate matter at the top of the bed might also explain the slower rates of rNV deposition (*13*). Enhanced deposition near the filter outlet could be due to more favorable rNV interactions with deposited wastewater particles, as would occur in the early stages of filter ripening (*10*). The higher filtration rates may also be due to a modification of the rNV particles that occurs after exposure to wastewater. For example, the coagulation of rNV particles with particulate organic matter in the wastewater could lead to accelerated filtration in the bottom half of the filter where organic surface coatings are less abundant. Divalent cations in the wastewater could also specifically adsorb to the virus surface and reduce its surface charge (*62*, *63*), although this effect was not seen in the electrophoretic mobility measurements of the rNV particles in wastewater (Table 1).

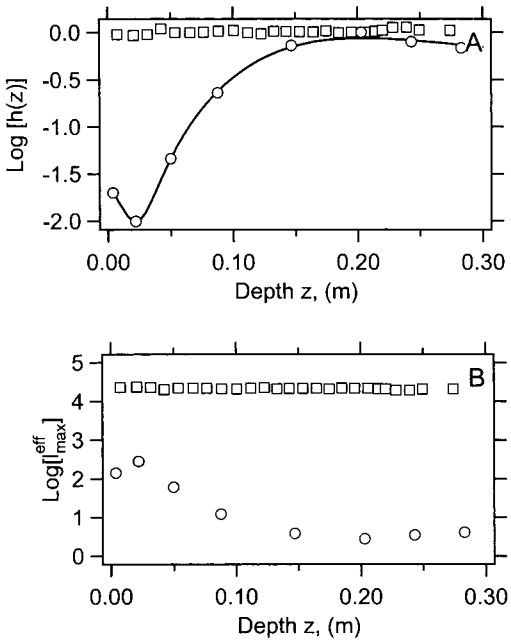

FIGURE 2. Values of the macroscale heterogeneity function calculated from the spatial pattern of deposited particles (A) and the corresponding effective maximum length scale (B) for filtration experiments conducted with 0.01 M NaCl solution (□) and wastewater (○). For the wastewater experiment, the following empirical function was fitted to the macroscale heterogeneity function (plotted as a solid line in panel A), $h(z) = a_1 z + a_2(1 + a_3/a_2 + \text{erf}[(z - a_4)/a_5])$, where $a_1 = -2.28$, $a_2 = 0.69$, $a_3 = 0.0045$, $a_4 = 0.11$, and $a_5 = 0.073$. These fitting coefficients were determined using a Levenbert–Marquardt nonlinear least-squares approach (*73*).

To determine if our modified equations can accurately model both the spatial pattern of retained rNV particles and the observed effluent levels, we fit the wastewater $h(z)$ profile with an empirical expression (solid line in Figure 2A, see figure legend) and then used the resulting mathematical description for $h(z)$ to calculate $C(z)$ and $S(z)$ from eqs 8a and 8b, respectively. The model fit for $S(z)$ and $C(z)$, shown as solid lines in panels A and C, respectively, of Figure 1,

match the observed data remarkably well. The model fit for $C(L)$ plotted in Figure 1A was corrected to account for the imperfect recovery of particles in this experiment (eq 7).

Limitations of the Power-Law Filtration Model. The filtration model presented here has a number of limitations that merit further investigation. To fit the model to experimental data, three separate variables were adjusted: the minimum and maximum filtration length scales l_{min} and l_{max} and the slope of the log−log retained particle profile a. The value of l_{min} was estimated by assuming diffusion-limited deposition (see eq 6a), whereas both l_{max} and a were determined by fitting experimental data for S and C. Ideally, the values of l_{max} and a could be computed from first principles for a given system, although no procedure for doing so is provided in this paper. Our model also fails to account for the dynamic evolution of deposition kinetics that accompanies continuous filter operation. In principle, dynamic processes, such as ripening and blocking, could be incorporated into the formulation of l_{max}, but these refinements are not explored here.

Implications for Potable Reuse. The data and modeling presented in this paper demonstrate that microscale and macroscale heterogeneities profoundly affect the kinetics of particle filtration. Furthermore, the inclusion of heterogeneity in filtration models has significant policy ramifications for the potable reuse of wastewater. If we just consider the effects of microheterogeneity, for example, then the differences between filtration levels predicted by eqs 4 and 5 grow exponentially with distance if $a > 1$. Even if $a < 1$, as it is for the NaCl filtration experiments described in this paper, the differences in filtration predicted by the two models can be enormous. If we accept a 1% lifetime risk for microbial infection and a 10^{-5} risk of death from drinking water (*64*), then the concentration of viruses in drinking water should not exceed 2×10^{-7} viruses/L (*65*). Assuming a starting virus concentration in wastewater of 10^4/L, this implies that the virus concentration should be reduced by 11 $\log_{10}$ units during the treatment process—the so-called 11 $\log_{10}$ rule (*66*). Assuming that filtration is the only barrier to virus transmission (which is generally not the case, see below) and using the filtration length scale $l = 1.7$ m estimated from the breakthrough curves in Figure 1A, the standard model predicts that this level of removal is achieved if the sand filter is 43 m long. Although a filter of this length is not practical in an above-ground treatment process, 43 m would be a reasonable set-back distance between a recharge basin employing untreated wastewater and a groundwater production well. In contrast, our microscale heterogeneity model of filtration (eq 8a) with values of $l_{min} = 10^{-2.88}$ m and $l_{max} = 10^{4.34}$ m estimated from the NaCl experiment predicts that the same degree of removal is achieved only if the filter is ~10000 times longer. A set-back distance closer to the exponential model prediction, 56 m, is expected if both microscale and macroscale heterogeneities are operative and we use the parameter values estimated from the wastewater experiment, holding $h(z) = 1$ in the far field.

In practice, other factors besides filtration also affect the fate and transport of viruses in the subsurface, including virus inactivation (*67*) and dilution of the viral plume with ambient groundwater by hydrodynamic dispersion (*68*). In above-ground treatment systems, additional processes are employed to remove viruses, including disinfection with chemical agents or UV light, flocculation/sedimentation, and membrane filtration technologies (*69*). The relatively slow rate of removal predicted by power-law filtration and the uncertain spatial variability in filtration rates caused by macroscale heterogeneity place a greater burden on these other processes as the primary barriers to microbial pathogens. Previous field investigations have noted that viruses can travel over large distances, as much as 1 km (*26*, *70*). The rapid movement of viruses through the subsurface over large distances is consistent with a power-law description of filtration.

Acknowledgments

This study was funded by grants from the NSF/EPA Water and Watersheds Program (R824770), from the Orange County Water District (OCWD-25736), and from the National Water Research Institute (EM 699-630-99). We gratefully acknowledge wastewater analyses performed by the Los Angeles County Sanitation Districts. We thank William Yanko, Jeff Kuo, Brett Sanders, and Ronald Linsky for helpful comments on the manuscript.

Supporting Information Available

Procedure for collecting the wastewater samples as well as descriptions of the physical and chemical analyses and the derivation of eq 7. This material is available free of charge via the Internet at http://pubs.acs.org.

Literature Cited

(1) *Issues in Potable Reuse*; National Research Council; National Academy Press: Washington, DC, 1998; p 14−44, 74−117.
(2) Drinking Water; National Primary Drinking Water Regulations; Filtration, Disinfection; Turbidity, *Giardia lamblia*, Viruses, *Legionella*, and Heterotrophic Bacteria: Final Rule, U.S. EPA. *Fed. Regist.* **1989**, *54* (June 29), 27486.
(3) Drinking Water; National Primary Drinking Water Regulations; Total Coliforms (including Fecal Coliforms and *E. coli*): Final Rule, U.S. EPA. *Fed. Regist.* **1989**, *54* (June 29), 27544.
(4) Iwasaki, T. *J. Am. Water Works Assoc.* **1937**, *29*, 1591.
(5) Yao, K.-M.; Habibian, M. T.; O'Melia, C. R. *Environ. Sci. Technol.* **1971**, *5*, 1105.
(6) Sim, Y.; Chrysikopoulos, C. V. *Water Resourc. Res.* **1995**, *31*, 1429.
(7) Sim, Y.; Chrysikopoulos, C. V. *Trans. Porous Media* **1998**, *30*, 87.
(8) Corapcioglu, M. Y.; Haridas, A. *Adv. Water Res.* **1985**, *8*, 188.
(9) Tobiason, J. E. *Colloids Surf.* **1989**, *39*, 53.
(10) Darby, J. L.; Lawler, D. F. *Environ. Sci. Technol.* **1990**, *24*, 1069.
(11) Tobiason, J. E.; Vigneswaran, B. *Water Res.* **1994**, *28*, 335.
(12) Hunt, J. R.; Hwang, B.-C.; McDowell-Boyer, L. M. *Environ. Sci. Technol.* **1993**, *27*, 1099.
(13) Johnson, P. R.; Elimelech, M. *Langmuir* **1995**, *11*, 801.
(14) Ko, C.-H.; Elimelech, M. *Environ. Sci. Technol.* **2000**, *34*, 3681.
(15) Albinger, O.; Biesemeyer, B. K.; Arnold, R. G.; Logan, B. E. *FEMS Microbiol. Lett.* **1994**, *124*, 321.
(16) Baygents, J. C.; Glynn, J. R.; Albinger, O.; Biesemeyer, B. K.; Ogend, K. L.; Arnold, R. G. *Environ. Sci. Technol.* **1998**, *32*, 1596.
(17) Camesano, T. A.; Logan, B. E. *Environ. Sci. Technol.* **1998**, *32*, 1699.
(18) Harter, T.; Wagner, S.; Atwill, E. R. *Environ. Sci. Technol.* **2000**, *34*, 62.
(19) Gerba, C. P.; Lance, J. C. *Appl. Environ. Microbiol.* **1978**, *36*, 247.
(20) Bales, R. C.; Li, S.; Maguire, K. M.; Yahya, M. T.; Gerba, C. P.; Harvey, R. W. *Ground Water* **1995**, *33*, 653.
(21) Bales, R. C.; Li, S.; Yeh, T. C. J.; Lenczewski, M. E.; Gerba, C. P. *Water Resourc. Res.* **1997**, *33*, 639.
(22) Pieper, A. P.; Ryan, J. N.; Harvey, R. W.; Amy, G. L.; Illangasekare, T. H.; Metge, D. W. *Environ. Sci. Technol.* **1997**, *31*, 1163.
(23) Schijven, J. F.; Hoogenboezem, W.; Nobel, P. J.; Medma, G. J.; Stakelbeek, A. *Water Sci. Technol.* **1998**, *38*, 127.
(24) DeBorde, D. C.; Woessner, W. W.; Kiley, Q. T.; Ball, P. N. *Water Res.* **1999**, *33*, 2029.
(25) Schijven, J. F.; Hoogenboezem, W.; Hassanizadeh, S. M.; Peters, J. H. *Water Resourc. Res.* **1999**, *35*, 1101.
(26) Schijven, J. F.; Hassanizadeh, S. M. *Crit. Rev. Environ. Sci. Technol.* **2000**, *30*, 49.
(27) Swanton, S. W. *Adv. Colloid Interface Sci.* **1995**, *54*, 129.
(28) Ryan, J. N.; Elimelech, M. *Colloids Surf. A* **1996**, *107*, 1.
(29) Song, L.; Elimelech, M. *J. Colloid Interface Sci.* **1994**, *167*, 301.
(30) Song, L.; Johnson, P. R.; Elimelech, M. *Environ. Sci. Technol.* **1994**, *28*, 1164.
(31) Bowen, B. D.; Epstein, N. *J. Colloid Interface Sci.* **1979**, *72*, 81.
(32) Bhattacharajee, S.; Ko, C.-H.; Elimelech, M. *Langmuir* **1998**, *14*, 3365.
(33) Elimelech, M.; Nagai, M.; Ko, C.-H.; Ryan, J. N. *Environ. Sci. Technol.* **2000**, *34*, 2143.

(34) Hedberg, C. W.; Osterholm, M. T. *Clin. Microbiol. Rev.* **1993**, *6*, 199.
(35) Estes, M. K.; Hardy, M. E. In *Infections of the Gastrointestinal Tract*; Raven Press: New York, 1995.
(36) Fankhauser, R. L.; Noel, J. S.; Monroe, S. S.; Ando, T.; Glass, R. I. *J. Infect. Dis.* **1998**, *178*, 1571.
(37) Jiang, X.; Graham, D. Y.; Wang, K.; Estes, M. K. *Science* **1990**, *250*, 1580.
(38) Prasad, B. V.; Rothnagel, R.; Jiang, X.; Estes, M. K. *J. Virol.* **1994**, *68*, 5117.
(39) Hardy, M. E.; Tanaka, T. N.; Kitamoto, N.; White, L. J.; Ball, J. M.; Jiang, X.; Estes, M. K. *Virology* **1996**, *217*, 252.
(40) Herrmann, J. E.; Blacklow, N. R.; Matsui, S. M.; Lewis, T. L.; Estes, M. K.; Ball, J. M.; Brinker, J. P. *J. Clin. Microbiol.* **1995**, *33*, 2511.
(41) Hardy, M. E.; White, L. J.; Ball, J. M.; Estes, M. K. *J. Virol.* **1995**, *68*, 1693.
(42) Kapikian, A. K.; Estes, M. K.; Chanock, R. M. In *Fields Virology*, 3rd ed.; Raven Publishers: Philadelphia, PA, 1996.
(43) Prasad, B. V. V.; Hardy, M. E.; Dokland, T.; Bella, J.; Rossmann, M. G.; Estes, M. K. *Science* **1999**, *286*, 287.
(44) Redman, J. A.; Grant, S. B.; Olson, T. M.; Hardy, M. E.; Estes, M. K. *Environ. Sci. Technol.* **1997**, *31*, 3378.
(45) Bak, P. *How Nature Works*; Copernicus: New York, 1996.
(46) Logan, B. E. *Environmental Transport Processes*; Wiley: New York, 1999; pp 564−613.
(47) Elimelech, M.; Gregory, J.; Jia, X.; Williams, R. *Particle Deposition and Aggregation*; Butterworth Heinemann: Oxford, U.K., 1995.
(48) Happel, J. *AIChE J.* **1958**, *4*, 197.
(49) Litton, G. M. Ph.D. Thesis, University of California, Irvine, CA, 1993; pp 67−68.
(50) Litton, G. M.; Olson, T. M. *Environ. Sci. Technol.* **1993**, *27*, 185.
(51) Amirbahman, A.; Olson, T. M. *Colloids Surf. A* **1995**, *99*, 1.
(52) Liu, D.; Johnson, P. R.; Elimelech, M. *Environ. Sci. Technol.* **1995**, *29*, 2963.
(53) Elimelech, M.; O'Melia, C. R. *Environ. Sci. Technol.* **1990**, *24*, 1528.
(54) Darby, J. L.; Lawler, D. F.; Wilshusen, T. P. *J. Water Pollut. Control Fed.* **1991**, *63*, 228.
(55) Clark, S. C.; Lawler, D. F.; Cushing, R. S. *J. Am. Water Works Assoc.* **1992**, *84* (12), 61.
(56) Tobiason, J. E.; Johnson, G. S.; Westerhoff, P. K.; Vigneswaran, B. *J. Environ. Eng.* **1993**, *119*, 520.
(57) Ruckenstein, E., Prieve, D. C. *AIChE J.* **1976**, *22*, 276.
(58) Israelachvili, J. N. *Intermolecular and Surface Forces*, 2nd ed.; Academic Press: San Diego, CA, 1992.
(59) Kreyszig, E. *Advanced Engineering Mathematics*, 7th ed.; Wiley: New York, 1993; pp 957−958.
(60) Gabellini, Y.; Meunier, J.-L. *J. Phys. A* **1992**, *25*, 3683.
(61) Broide, M. L.; Cohen, R. J. *J. Colloid Interface Sci.* **1992**, *153*, 493.
(62) Kamel, A. A.; Ma, C. M.; El-Aasser, M. S.; Micale, F. J.; Vanderhoff, J. W. *J. Disp. Sci. Technol.* **1981**, *2*, 315.
(63) Zukoski, C. F.; Saville, D. A. *J. Colloid Interface Sci.* **1986**, *114*, 32.
(64) Bennet, J. V.; Holmberg, S. D.; Rogers, M. F.; Solomon, S. L. In *Closing the Gap: The Burden on Unnecessary Illness*; Amler, R. R., Dull, H. B., Eds.; Oxford University Press: New York, 1987.
(65) Regli, S.; Rose J. B.; Haas, C. N.; Gerba, C. P. *J. Am. Water Works Assoc.* **1991**, *83*, 76.
(66) Grubbs, T. R.; Pontius, F. W. *J. Am. Water Works Assoc.* **1992**, *84*, 25.
(67) Yates, M. V.; Gerba, C. P.; Kelley, L. M. *Appl. Environ. Microbiol.* **1985**, *49*, 778.
(68) Rehmann, L. L. C.; Welty, C.; Harvey, R. W. *Water Resourc. Res.* **1999**, *35*, 1987.
(69) Tchobanoglous G.; Burton, F. L. *Wastewater Engineering: Treatment, Disposal, and Reuse*; McGraw-Hill: New York, 1991.
(70) Gerba, C. P. In *Groundwater Pollution Microbiology*; Bitton, G., Gerba, C. P., Eds; Wiley: New York, 1984; p 225.
(71) Redman, J. A.; Grant, S. B.; Olson, T. M.; Adkins, J. A.; Jackson, J. L.; Castillo, M. S.; Yanko, W. A. *Water Res.* **1998**, *33*, 43.
(72) Folk, R. L. *Petrology of Sedimentary Rocks*; Hemphill Publishing: Austin, TX; pp 29−61.
(73) Press, W. H.; Flannery, B. P.; Teukolsky, S. A.; Vetterling, W. T. *Numerical Recipes*; Cambridge University Press: New York, 1986.

Received for review March 14, 2000. Accepted February 5, 2001.

ES0010960